

Er:YAG POLYCRYSTALLINE CERAMICS: USE OF SiO_2 AND B_2O_3 AS SINTERING ADDITIVES AND THEIR EFFECTS ON THE OPTICAL AND STRUCTURAL PROPERTIES

CERÁMICAS POLICRISTALINAS DE Er:YAG. EL USO DE SiO_2 Y B_2O_3 COMO ADITIVOS DE SINTERIZACIÓN Y SUS EFECTOS EN LAS PROPIEDADES ÓPTICAS Y ESTRUCTURALES

L. MOREIRA^{a,b}, L. PONCE^{a†}, E. DE POSADA^a, T. FLORES^a

a) Instituto Politécnico Nacional Cicata Altamira, Altamira, Tamps., Mexico 89600

b) TECNO-INSPEC S.A. de C.V., Tampico, Tamps., Mexico 89260; guira_98@yahoo.com[†]

† corresponding author

Recibido 21/3/2017; Aceptado 23/10/2017

The effects of SiO_2 and B_2O_3 as sintering additives on the optical and structural properties of Er:YAG polycrystalline ceramics sintered without additional external pressure and in a high vacuum were investigated. The optimum optical and structural properties were obtained by doping the ceramics with 0.5% of SiO_2 and 0.17 wt. % of SiO_2 , and 0.33 wt. % of B_2O_3 ($\text{B}^{3+}:\text{Si}^{4+} = 2.0$), respectively, with the former giving the better results. Alternatively, it is shown that through the addition of B_2O_3 , it is possible to reduce the sintering temperature and obtain good density values.

En el trabajo se investigan los efectos de aditivos de sinterización como el SiO_2 y el B_2O_3 , en las propiedades ópticas y estructurales de cerámicas policristalinas de Er:YAG sinterizadas en alto vacío sin aplicar presión externa. La mejor calidad óptica y estructural se obtuvo dopando las cerámicas con 0.5% de SiO_2 , 0.17% de SiO_2 and 0.33% de B_2O_3 ($\text{B}^{3+}:\text{Si}^{4+} = 2.0$) respectivamente. Por otra parte, se demuestra que con la adición de B_2O_3 es posible reducir la temperatura de sinterizado y obtener valores de densidad adecuados.

PACS: Microstructure crystals, 61.72.-y; Ceramics fabrication, 81.05.Je, 81.05.Mh; Laser materials, 42.70.Hj

I. INTRODUCTION

Yttrium aluminum garnet (YAG) is one of the most attractive and studied materials for laser applications due to its excellent optical, thermal, mechanical and spectroscopic properties [1,2]. Because of its birefringence-free cubic crystal structure, transparent polycrystalline ceramics with densities of up to 99.99% can be produced by sintering.

The manufacturing of translucent ceramics started in the 1950s. Coble was the first to demonstrate that ceramics could be sintered to a translucent/transparent state with high densities, thus reducing or eliminating light scattering from residual porosity and second phases [3,4]. This, along with the discovery of the ruby laser in 1960 [5] allowed Hatch et al. [6] to start using $\text{Dy}^{2+}:\text{CaF}_2$ ceramics in cryogenic conditions as an active laser medium in 1964. For four decades, ceramics were used in laser applications, however, their optical properties and laser efficiency could not achieve the desired values [7,8]. In 1995, Ikesue et al. [9] first reported Nd:YAG transparent polycrystalline ceramics with a high laser efficiency fabricated by sintering mixed Y_2O_3 , Al_2O_3 and Nd_2O_3 powders at 1750°C for 8 h. They found that adding SiO_2 as a sintering additive was critical to sintering transparent Nd:YAG, proposing that SiO_2 plays a key role in the incorporation of Nd^{3+} ions into the YAG lattice. Afterwards, Yagi et al. [10,11] developed another method to obtain Nd:YAG transparent ceramics by sintering co-precipitated Nd:YAG nanometric powder doped with SiO_2 at 1700°C. With these methods, several transparent

ceramics, such as Nd:YAG [12], Er:YAG [2] and Yb:YAG [13], have been fabricated.

In 2007, Sallé et al. [14] noted that small silica additions improved the densification kinetics and inhibited abnormal grain growth in the final sintering stage. Boulesteix et al. [15], using SiO_2 as a sintering additive, demonstrated the liquid-phase sintering mechanisms in Nd:YAG [16] and revealed that when obtaining Nd:YAG ceramics, SiO_2 addition increased Nd^{3+} diffusion tenfold [15]. Other reports have shown the beneficial effects of SiO_2 in the sintering process due to the increase in the grain boundary diffusion coefficient or the decrease in grain boundary surface energy in the presence of second phases [17–19], indicating that the effect of silica is also linked to the formation of a solid solution by replacing Al^{3+} with Si^{4+} at the tetrahedral sites. Such a transformation leads to Y^{3+} vacancy formation that can improve the network diffusion coefficient, therefore improving the YAG densification kinetics. It is clear that SiO_2 acts as a transient liquid-phase sintering additive during YAG sintering. Specifically, a liquid-phase is formed at 1390°C and affects densification in intermediate states, followed by the replacement of Si^{4+} within the YAG lattice, leading to densification by solid-state mechanisms.

Even though the important contribution of SiO_2 as a sintering additive has been recognized, it has also been identified as the cause of optical defects, including second phase particles [15] and color centers in ceramics and monocrystals [20]. Also, after the annealing process there are always Si-rich particle phases in YAG ceramics doped with SiO_2 , which affects their

transparency [21]. In addition, Si-rich particle phases tend to precipitate from YAG ceramics at high temperatures for a prolonged period of time [22].

Thus, minimizing the sintering additives used in the ceramic process continues to be a challenge [23]. Recently, Stevenson et al. [24] obtained Nd:YAG transparent ceramics doped with B_2O_3 - SiO_2 , in which the SiO_2 levels were reduced to 0.112%. Alternatively, using B_2O_3 in glass ceramics allows densification to occur before crystallization [25], thereby decreasing the crystallization temperature [26] and promoting nucleation [27]. Similarly, in spinel-type ceramics, B_2O_3 has proven to be useful in obtaining adequate transparency [28]. Based on the above, and considering that we could not find any previous studies regarding the use of B_2O_3 in Er:YAG ceramics and that there are few reports regarding SiO_2 as a sintering additive, the present work studies the effect of SiO_2 and B_2O_3 , when used as sintering additives, on the optical and structural properties of Er:YAG ceramics.

II. EXPERIMENTAL

The raw materials used to obtain Er:YAG ceramics through a solid-state reaction and vacuum sintering were high-purity commercial powders of $\alpha-Al_2O_3$ (> 99.99%, $D_{50} \approx 1125$ nm, Baikowski Japan Co, LTD, Chiba, Japan), Y_2O_3 (> 99.99%, $D_{50} \approx 1115$ nm, Baikowski Japan Co, LTD, Chiba, Japan) and Er_2O_3 (> 99.99%, $D_{50} \approx 50$ nm, Sigma-Aldrich, USA). As sintering additives, tetraethyl orthosilicate (TEOS, > 99.999%, Sigma-Aldrich, USA) and trimethyl borate (TRBO, > 99.5%, Sigma-Aldrich, USA) were used as SiO_2 and B_2O_3 , respectively. Oxide powders and sintering additives were mixed in stoichiometric proportions of 2.0 at. % of Er:YAG with 0.5 wt. % of TEOS as a sintering aid. The resulting powders were synthesized and a green compact was formed, according to a procedure described elsewhere [29].

The obtained green compacts were sintered in a high vacuum ($< 10^{-3}$ Pa) at 1550°C for 12 h using an oven designed and built for this purpose [29]. In order to study the sintering kinetics, the green compacts were sintered at three different temperatures for 12 h: 1450, 1500 and 1550°C.

The ceramic microstructures were observed by scanning electron microscopy (SEM, model JSM-7500F, JEOL, USA) and atomic force microscopy (AFM, model TT-AFM, AFM Workshop, USA). For the SEM measurements, ceramics were previously polished using an accelerating voltage of 3.0 kV. AFM measurements were made before and after polishing. Each sample was analyzed in three different areas with a scanning area of $40 \times 40 \mu m^2$. The densities of the ceramics were measured using the Archimedes' method, using deionized water as an immersion medium. Determination of the grain size of the sintered samples was carried out using the linear intercept method [30]. The mean grain size was calculated by multiplying the average linear intercept distance by 1.56 [31].

X-ray diffraction (XRD) was performed using the grazing incidence configuration with the incident beam at 1.5° (X

Pert PRO MRD, PANalytical).

Transmittance of the Er:YAG ceramics was measured by a USB4000+ spectrometer, supplied by Ocean Optics with a tungsten halogen light source (360–2400 nm, model LL, Ocean Optics, USA).

III. RESULTS AND DISCUSSION

III.1. Powder preparation

In our previous work [29], it was demonstrated that the bimodal distribution of the starting powder particles further improves, compared with monomodal distributions, the density of Er:YAG ceramics and thus, their structural and optical properties. The optimum result was obtained for the bimodal distribution resulting from mixing two monomodal distributions (1:4) with an average particle size ratio of 2:1.

On this basis, synthesized powders were processed in order to obtain, for each one, a grain size distribution according to the particle size distribution (Figure 1). For this, powders were selected using sieves of 200, 250 and 325 mesh. We obtained two powder partial distributions for each synthesized powder: P1 were those between 200 and 250 mesh, and P2 were those between 250 and 325 mesh. Both P1 and P2 experienced an average size ratio of $SiO_2/m2 : 1$. Finally, partial distributions were mixed in a 1:4 ratio, resulting in the starting powders used in each sample of interest.

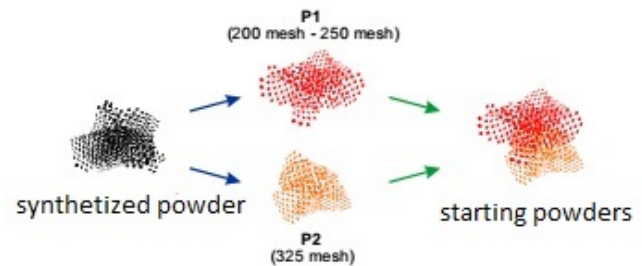


Figure 1. Process for obtaining the final powders required to fabricate Er:YAG ceramics from two partial distributions of the resulting powders synthesized from oxides and initial additives.

Table 1. Samples with their respective wt. % used.

Sample	TEOS (wt. %)
T00	0.0
T02	0.2
T03	0.3
T04	0.4
T05	0.5
T06	0.6

III.2. SiO_2 and its effect on Er:YAG ceramics

SiO_2 is crucial for the ceramic sintering process for optical applications, however, there are few studies reporting its effect on the structure and optical properties of Er:YAG

ceramics. This is also a starting point to study the influence of $B_2O_3-SiO_2$ on such properties. Table 1 shows a summary of the samples and additives used. For nomenclature purposes, samples were classified with numbers and letters, letters stand for additives, which in this case is TEOS, and the number represents the quantity in wt. % that was used.

Figure 2 shows the XRD pattern of sample T00 after sintering at $1550^\circ C$ for 12 h. As shown, the characteristic peaks of the ceramics can be indexed to the YAG garnet-like cubic structure (YAG, ICSD: 98-004-1144). The same result was obtained for each sample. Thus, we can conclude that complete YAG transformation occurred during the vacuum sintering process, regardless of the quantity of additive used.

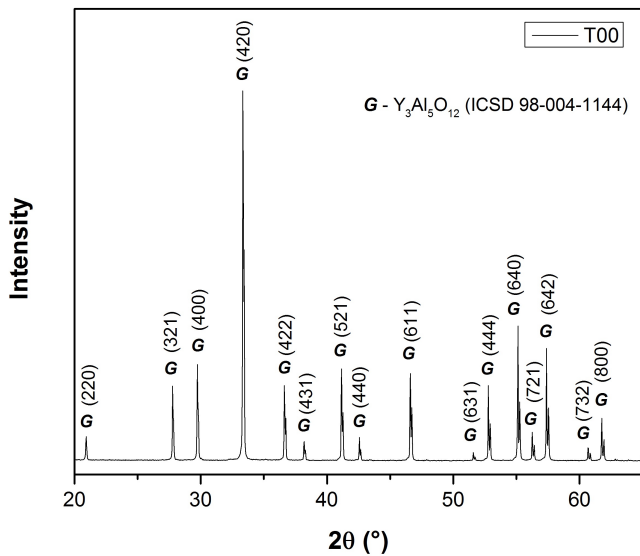


Figure 2. XRD pattern of the ceramic sample T00 sintered at $1550^\circ C$ for 12 h. The identified phase is G ($Y_3Al_5O_{12}$).

Figure 3 shows the behavior of the relative density of ceramic samples T00 to T06. An increase in the TEOS concentration causes higher densification of the ceramics, with samples T05 (94.95 %) and T06 (95.00 %) having the highest densities. Even though sample T06 with 0.06 wt. % TEOS is the densest, there is only a slightly difference when compared with sample T05 with 0.05 % TEOS. The rest of the samples experience different behavior. Sample T00, which was sintered without any additive, is the least dense.

Figure 4 shows the transmittance of ceramic samples T00 to T06 in terms of their respective relative densities. The results show an increase of transmittance with the improvement of the ceramics' relative density. With the exception of sample T06 and based on the results shown in Figure 3, an increase in the TEOS concentration results in better optical properties. This result is consistent with previous studies of Nd:YAG ceramics [19]. Sample T05 presents the best transmittance, and the obtained value is similar to the one reported by Ikesue et al. [32].

Sample T06, despite it was the densest, its transmittance was the highest. Note the direct relationship between the ceramics' density and its optical properties, considering that

density is related to the elimination of porosity in compact powders in order to form a solid material that is essentially pore-free, since these are a fundamental source of light scattering [30].

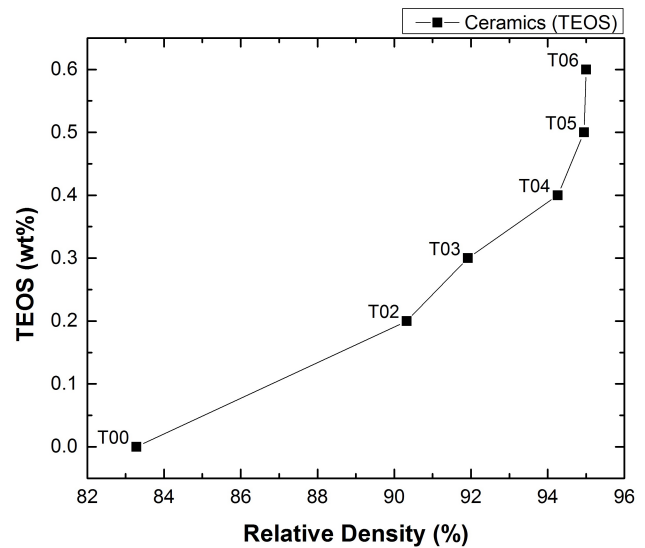


Figure 3. Relative density of ceramic samples T00 to T06 sintered at $1550^\circ C$ for 12 h.

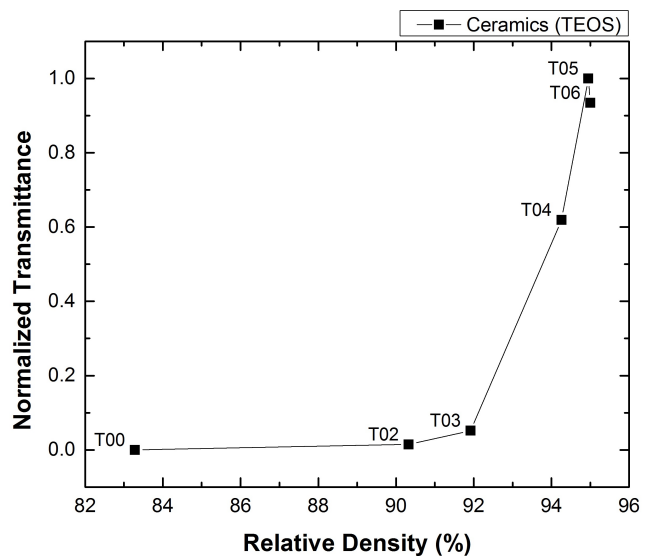


Figure 4. Transmittance of samples T00 to T06 in terms of relative density, sintered at $1550^\circ C$ for 12 h.

Figure 5a shows the AFM images of samples T00, T05 and T06 after being polished. Regarding the less dense sample T00 (Figure 3), its structure shows a marked increase in grain growth, characterized by heterogeneous microstructures, in which there are no sintering additives. Samples T05 and T06 present a more homogeneous grain structure and a better conformation can be observed. Even though sample T06 presents better results, some asymmetry in the structure can be observed and it is characterized by larger grains in the lower half and smaller grains towards the upper half. This behavior is not observed in any other sample. Figure

5b shows the grain size distribution. From their calculated geometric standard distributions (GSD), ρ_g , which give a measure of grain-size homogeneity, an improvement in the structure with an increase in the concentration of TEOS can be observed. Regarding the shape of the size distributions, for sample T06, there is a marked bimodal distribution, in which the transition between large and medium is not entirely smooth. This can cause the formation of zones with greater and lesser density in the ceramic structure, therefore generating stress, resulting in a negative impact on the optical properties (Figure 4).

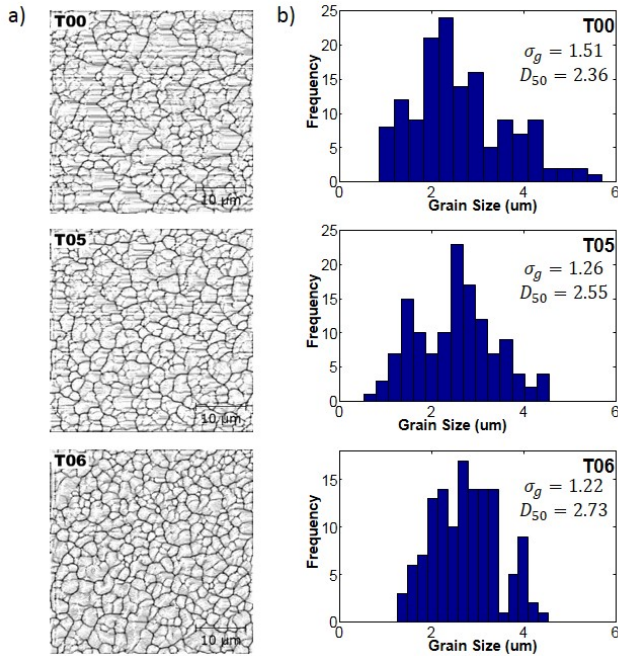


Figure 5. AFM images of ceramic samples T00, T05 and T06 sintered at 1550°C for 12 h and their respective grain size distributions. The analysis was carried out after the ceramics had been polished.

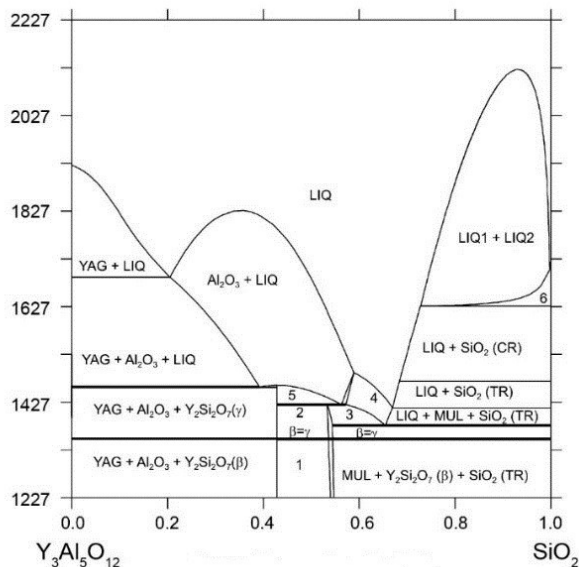


Figure 6. Phase diagram of $Y_3Al_5O_{12}-SiO_2$ [29].

According to the YAG-SiO₂ phases diagram [33] shown in

Figure 6, a liquid-phase is produced in the matrix of the YAG doped with SiO₂ above 1400°C. Thus, improvement in the density of ceramics doped with SiO₂ may be a consequence of the liquid-phase sintering, as proposed by Boulesteix et al. [16] in Nd:YAG ceramics.

Figure 7a and b shows the SEM images of ceramic samples T05 and T06, where the formation of Si-rich second phases can be observed, corresponding to 1: SiO₂ + Al₂O₃ and 2: SiO₂ + Y₂O₃ + Al₂O₃, and the main phase 3: Er_{0.06}Y_{2.94}Al₅O₁₂. The formed phases, as a consequence of the liquid-phase residues that are formed at temperatures over 1400°C [34], corroborate the Er:YAG ceramic densification by liquid-phase sintering mechanisms.

Even though Si-rich phases must activate and promote densification during sintering, an excess can affect the ceramics' optical properties [30]. In the case of ceramic T06 (Figure 7b), an excess of SiO₂ causes marked second phases with a higher concentration, which are the main cause of the detriment of the ceramics optical and structural properties (Figures 7a and 7b). Regarding sample T05 (Figure 7), despite presenting second phases, it also experiences the best transmittance. This result shows that it is possible to obtain ceramics with interesting optical properties even in the presence of second phases. A similar report has been published by Liu et al. [35] for Er:YAG ceramics.

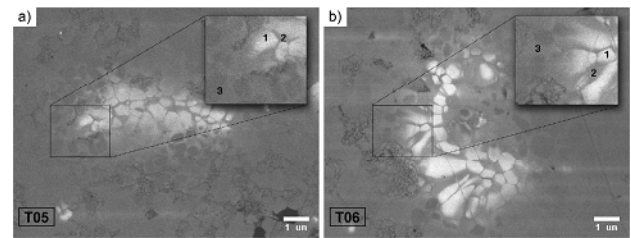


Figure 7. SEM images of ceramic samples T05 and T06 sintered at 1550°C for 12 h. The identified phases correspond to 1: SiO₂ + Al₂O₃, 2: SiO₂ + Y₂O₃ + Al₂O₃ and 3: Er_{0.06}Y_{2.94}Al₅O₁₂.

III.3. Influence of B₂O₃ on Er:YAG ceramic sintering

Even though the contribution of SiO₂ as a sintering additive is important, it has been proven to have secondary effects on the optical and structural properties of Er:YAG ceramics (Figure 7). In order to minimize the use of SiO₂, B₂O₃ was incorporated as a sintering additive using TRBO. For this, sample T05 was used as a reference, since it was the sample with the best optical properties and presented second phases in its structure.

For every sample, the total amount of additive was assumed to be equal to that of sample T05 at 0.5 wt. %. The TRBO:TEOS (B³⁺:S⁴⁺) ratio varied from 0.0 to 2.0. A certain nomenclature, consisting of one letter and two numbers, was used for samples doped with B₂O₃-SiO₂. Letter "B", indicates the presence of B₂O₃ as an additive, and the numbers indicate the B³⁺:S⁴⁺ ratio of sintering additives used in the sample. Thus, B₂0 represents a sample with 2 at. % Er:YAG with a B³⁺:S⁴⁺ ratio of 2.0 (0.33 wt. % TRBO:0.17 wt. % TEOS = 2.0).

Table 2 summarizes the characteristics of the samples used with the amount of sintering additives used.

Table 2. Composition of the samples using TEOS and TRBO as sintering additives for the fabrication of 2 at. % Er:YAG ceramics.

Sample	T05	B05	B10	B15	B20
Total: TEOS+	0.5	0.5	0.5	0.5	0.5
TEOS (wt. %)	0.50	0.33	0.25	0.20	0.17
TRBO (wt. %)	0.00	0.17	0.15	0.30	0.33
TRBO: TEOS	0.0	0.5	1.0	1.5	2.0

Figure 8 shows the relative density of the ceramics in terms of the $B^{3+}:S^{4+}$ ratio, whilst maintaining the total amount of additive equal to 0.5 wt. %. As observed, an increase in $B^{3+}:S^{4+}$ causes a progressive improvement of the ceramic's relative density. Using sample T05 as a reference, doped only with SiO_2 , with the increase of B_2O_3 and the decrease of SiO_2 , it starts to yield better results from the $B^{3+}:S^{4+}$ ratio = 0.25 : 0.25 = 1.0.

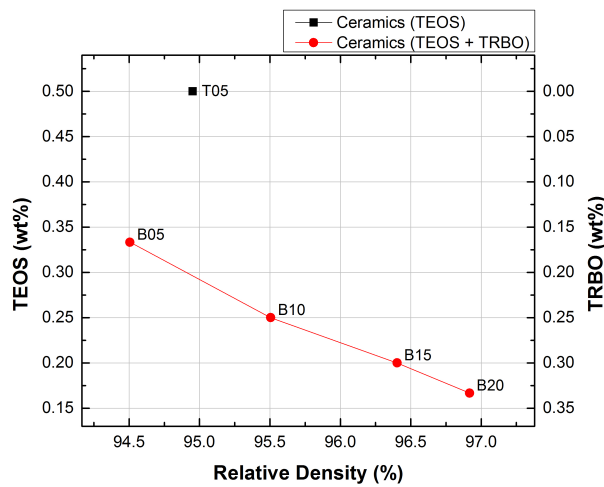


Figure 8. Density of the ceramics sintered at 1550°C for 12 h in terms of the Si^{4+} and B^{3+} concentration. The $B^{3+}:S^{4+}$ ratio varies from 0.0 to 2.0, whilst maintaining the total amount of additive equal to 0.5 wt. %.

Figure 9 shows AFM images of the ceramics after being polished and their respective grain size distributions. In Figure 9a, it can be observed that the structure becomes more uniform as the $B^{3+}:S^{4+}$ ratio increases. For the less-dense samples T05 and B06, some abnormal grain size growth was observed. This was more pronounced in the sample B05, which is the one with the lower density.

Using the results shown in Figure 9b, Figure 10 shows the GSD behavior and the average grain size of ceramics T05 and B05 to B20 in terms of their relative density. As can be observed, the average grain size varies from 2.29 to 3.00 μm , regardless of the ceramic's density value and the $B^{3+}:S^{4+}$ ratio. The GSD, opposite to the grain size behavior, decreases as the density and $B^{3+}:S^{4+}$ ratio increase. This result is consistent with the structure's homogeneity, which can be observed in Figure 9a. Ceramics B15 and B20 showed the best results, and were also the samples with the higher density and lower

amount of SiO_2 , respectively (Figure 8).

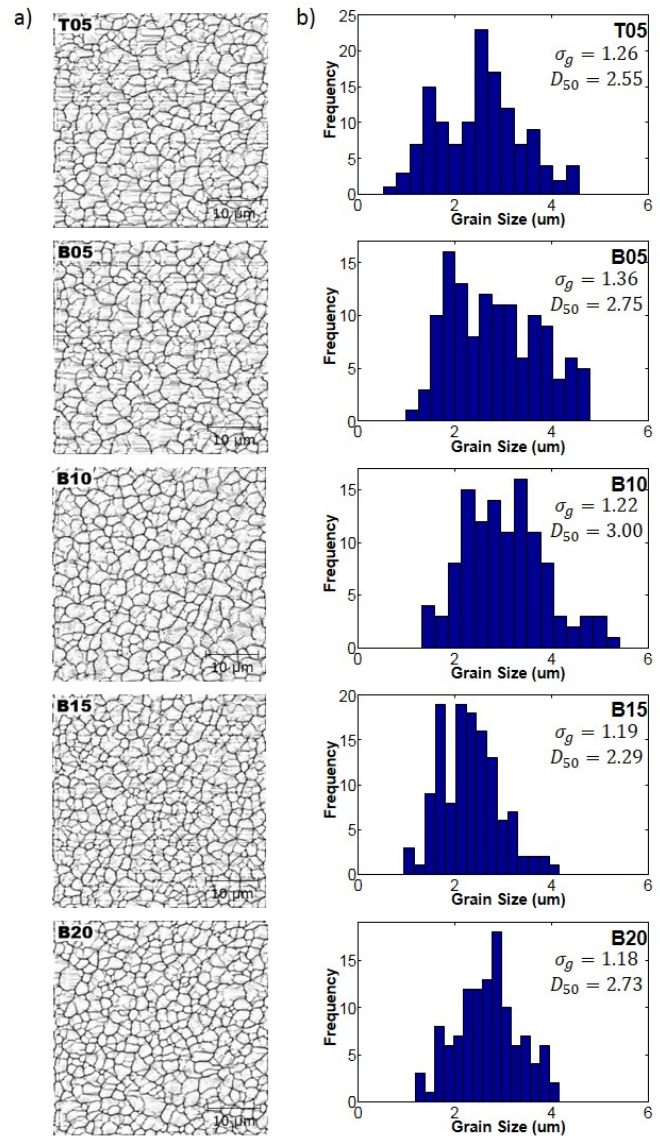


Figure 9. AFM images of ceramics T05 and B05 to B20 sintered at 1550°C for 12 h and their respective grain size distributions. The analysis was carried out after the ceramics had been polished.

Figure 11 shows the relative density of the ceramics sintered between 1450 and 1550°C for 12 h. The sintering kinetics at different temperatures reveal an increase in the densification of the samples doped with B_2O_3 (B05 to B20) regarding the sample doped only with SiO_2 (T05). At low temperatures, such as 1450 and 1500°C, the difference in the density between the samples doped with B_2O_3 and the sample doped only with SiO_2 becomes substantial. Using samples T05 and B20 as references, the difference in density corresponds to 13.00 %, 6.76 % and 1.97 % at 1450, 1500 and 1550°C, respectively. In optical terms, such differences are extremely decisive for the final optical properties [36,37]. Similarly, using B_2O_3 reduces the sintering temperature of the ceramics while maintaining or improving the ceramic's density values. Note that, for example, ceramic B20 obtained at 1450°C experienced a better density than ceramic T05 obtained at 1500°C. Also, ceramic B20 at 1500°C experienced similar densities to ceramics T05

and B05 sintered at 1550°C. In every case, the temperature difference is 50°C.

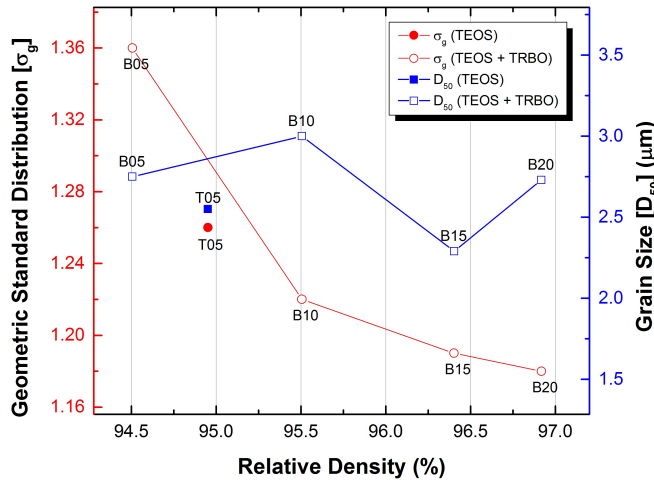


Figure 10. GSD (ρ_g) and average grain size (D_{50}) corresponding to ceramic samples T05 and B05 to B20 in terms of their respective relative densities.

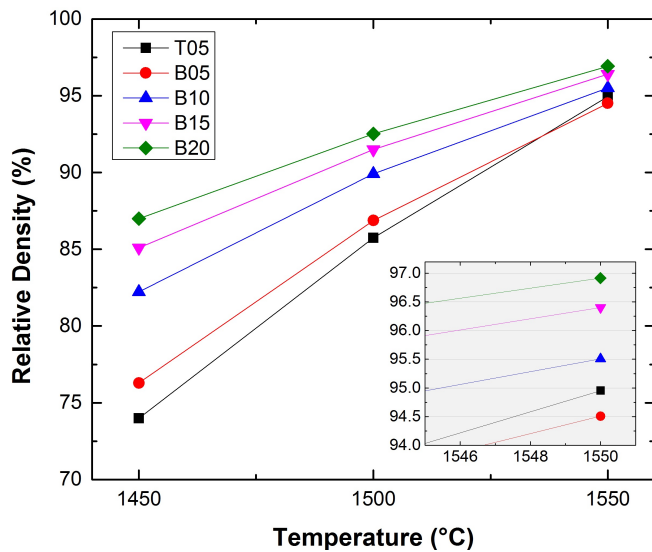


Figure 11. Relative density of ceramic samples T05 and B05 to B20, sintered for 12 h at different temperatures.

Figure 12 shows the normalized transmittance of ceramics T05 and B05 to B20 doped with SiO_2 , and $\text{B}_2\text{O}_3\text{-SiO}_2$ respectively. An increase in the $\text{B}^{3+}:\text{S}^{4+}$ ratio implies a considerable improvement in the ceramics' optical properties. This result is consistent with the values and behaviors of the densities shown in Figures 8 and 11, considering that a material's density is directly related to its porosity and, in turn, pores constitute the main source of light scattering in the material [9].

According to the literature [38], additives should reduce the anisotropy of crystal growth and make its shape more isometric. Otherwise, anisotropy would lead to the generation of tensile forces in the ceramics, causing inter-crystalline porosity. Note that the shape and homogeneous distribution of the grains (Figures 9 and 10) result in better optical properties (Figure 12) with the increase of the $\text{B}^{3+}:\text{S}^{4+}$ ratio.

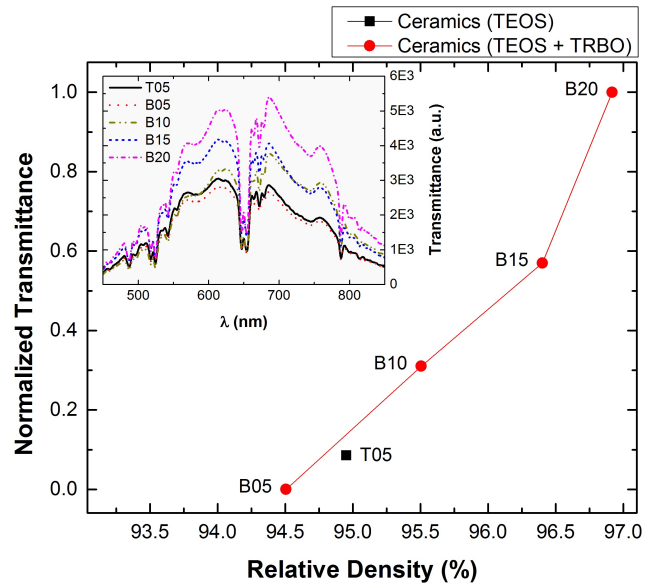


Figure 12. Normalized transmittance of the ceramics of 2 at. % Er:YAG, T05 and B05 to B20, doped with $\text{B}_2\text{O}_3\text{-SiO}_2$, and sintered at 1550°C for 12 h. The inserted graphic corresponds to the respective transmittance spectra of the ceramics within a spectral range of 450–850 nm.

Figure 13a–c shows the SEM images of ceramic samples T05, B10 and B20 after being polished and sintered at 1550°C for 12 h. As can be observed, for a total additive amount of 0.5 wt. %, an increase in the B_2O_3 amount and a decrease in the SiO_2 amount, results in the formation of less second phases in the ceramic structure. Thus, transmittance of the ceramics is favored (Figure 12), if we consider that grain boundary phases constitute one of the fundamental mechanisms that affect the ceramics' optical properties [39]. Figure 13d shows a SEM image of the sample B20 sintered at 1550°C for 18 h. Both, the amount and type of additives used and the sintering time, contribute to a better sintering process, where it is possible to obtain a homogeneous structure free of second phases.

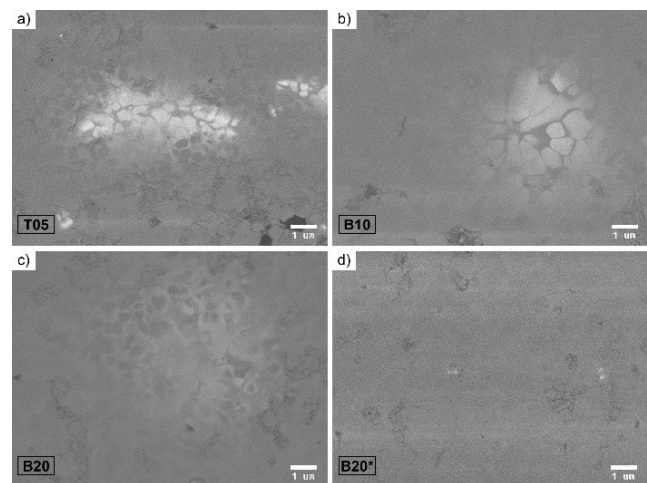


Figure 13. SEM images of the ceramic samples a) T05, b) B10 and c) B20 sintered at 1550°C for 12 h and d) ceramic B20* corresponding to sample B20 sintered at 1550°C for 18 h.

Figure 14 shows the substantial improvement of the optical properties of sample B20, with 0.33 wt. % TRBO and 0.17

wt. % TEOS, when sintered at 1550°C for 12 and 18 h, respectively.

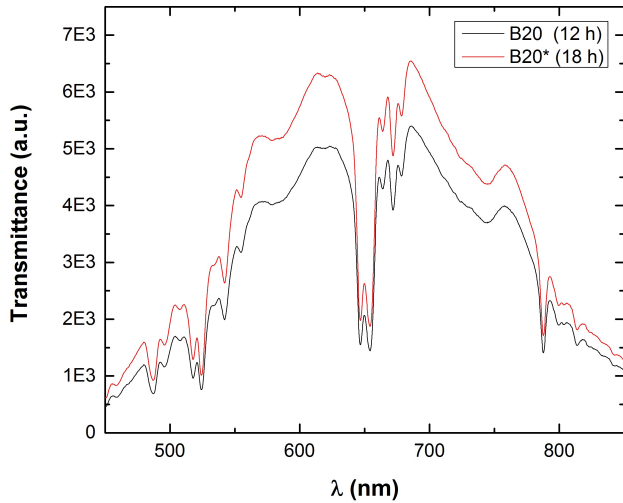


Figure 14. Transmittance of sample B20, sintered at 1550°C for 12 and 18 h, respectively.

In order to study the effect of sintering additives in the ceramics, an XPS analysis was carried out. Figure 15 shows the characteristic spectra of samples T05, B10 and B20, along with the wt.% of the representative components present in each sample shown in the table. In the case of Er(4d), Y(3d), Al(2p) and O(1s), fundamental components in the formation of Er:YAG ceramics, these remain virtually constant. Regarding Si(2p), its depletion is clearly shown as the $B^{3+}:S^{4+}$ ratio increases. In the case of B(1s), it cannot be detected, not even in ceramic B20, to which was initially added the highest amount of B_2O_3 prior to the sintering process (Table 2). This may be due to vaporization of B(1s) during the sintering process at 1550°C for 12 h. Other studies, in other circumstances, have also shown volatilization of B [40].

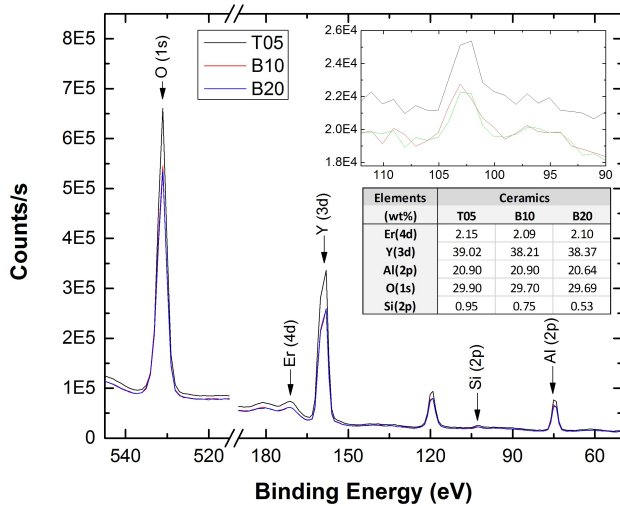


Figure 15. XPS spectra corresponding to ceramic samples B00, B10 and B20 sintered at 1550°C for 12 h.

B_2O_3 , among its physical properties, presents a melting point above 450°C [26]. In the sintering process of Er:YAG

ceramics using B_2O_3 - SiO_2 additives, the formation of Si-rich second phases was observed, which is typical in the liquid-phase sintering process (Figure 16). Alternatively, in the temperature range in which Er:YAG ceramics were sintered (1450–1550°C), the XPS analysis regarding the ceramics' composition never determined the presence of B(1s) in their structure once they were sintered at 1550°C for 12 h. As previously stated, the volatilization of B during the sintering process has been reported [40]. The previous work confirms the contribution of B_2O_3 - SiO_2 as sintering additives, which favors the liquid-phase sintering mechanisms.

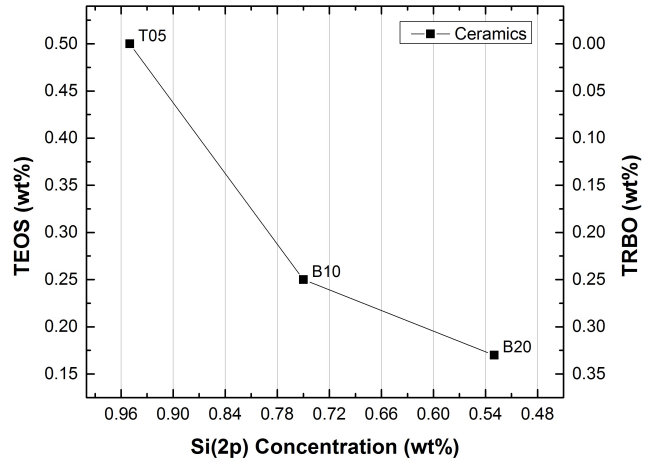


Figure 16. Si(2p) concentration in terms of the B_2O_3 :TEOS ratio in Er:YAG ceramics sintered at 1550°C for 12 h.

Know and Messing [41] created equation 2 to describe densification in diffusion limited densification in liquid phase sintering systems:

$$\frac{\partial \rho}{\rho_0 \partial t} \sim \frac{24\pi E(\rho) D_{liq} \delta_{liq}}{\beta_c^2 k_B T r^2} \quad (1)$$

where $E(\rho)$ is a density dependent function, D_{liq} the liquid phase constant, δ_{liq} the thickness of the liquid-phase layer, β_c the fractional area between particles, k_B the Boltzmann's constant, T the temperature and r the mean particle radius.

According to the Stokes-Einstein equation (2):

$$D_{liq} = \frac{k_B T}{6\eta r} \quad (2)$$

where D_{liq} is the diffusion constant for an ion diffusion in a liquid, η the viscosity and r is the atomic radius of the diffusing ion. Diffusion in a liquid is inversely proportional to the melting viscosity. Thus, an increase in densification and optical properties as a consequence of B^{3+} ions is related with decrease in viscosity in the liquid-phase during sintering, which, therefore, increases D_{liq} and the associated sintering kinetics by a liquid-phase sintering mechanism. Use of B_2O_3 as a sintering additive substantially contributes to the improvements of the Er:YAG ceramic's optical and structural properties.

IV. CONCLUSIONS

Using SiO₂ and B₂O₃ as sintering additives, Er:YAG polycrystalline ceramics were obtained. We demonstrate that the use of such additives in the manufacturing process of Er:YAG ceramics, sintered without external pressure and in high vacuum, substantially improves their structural and optical properties. The fundamental densification mechanism in ceramics is the liquid-phase sintering.

The use of B₂O₃ reduced the amount of SiO₂ additive and thus, the formation of Si-rich second phases that affect the ceramics' optical properties. Best optical and structural properties were obtained doping the ceramics with 0.5 % of SiO₂ and 0.17 wt. % of SiO₂, and 0.33 wt. % of B₂O₃ (B³⁺:Si⁴⁺=2.0), respectively.

Through the addition of B₂O₃, it is also possible to reduce the sintering temperature while obtaining good density values. In the studies made and for the temperature range used, a reduction of 50°C is reported resulting in similar or better density values.

ACKNOWLEDGMENTS

We acknowledge the SIP-IPN 2016-1804/0291 project and SIBE, EDI and SNI grants for financial support.

REFERENCES

- [1] J. Dong, A. Shirakawa, K.-i. Ueda, H. Yagi, T. Yanagitani, and A. A. Kaminskii, *Appl. Phys. Lett.* 89, 091114 (2006).
- [2] N. Ter-Gabrielyan, L. Merkle, E. Kupp, G. Messing, and M. Dubinskii, *Opt. Lett.* 35, 922 (2010).
- [3] R. Coble, *Am. Ceram. Soc. Bull.* 38, 507 (1959).
- [4] R. L. Coble, *J. Appl. Phys.* 32, 793 (1961).
- [5] T. H. Maiman, *Nature* 187, 493 (1960).
- [6] S. Hatch, W. Parsons, and R. Weagley, *Appl. Phys. Lett.* 5, 153 (1964).
- [7] C. Greskovich and J. Chernoch, *J. Appl. Phys.* 44, 4599 (1973).
- [8] C. Greskovich and J. Chernoch, *J. Appl. Phys.* 45, 4495 (1974).
- [9] A. Ikesue, Japanese patent 3 (1992).
- [10] Y. Takakimi, Y. Hideki, and Y. Hiroo, in *Japanese Patent* (1998).
- [11] T. Yanagitani, H. Yagi, and M. Ichikawa, in *Japanese Patent* (1998).
- [12] J. Liu et al., *Opt. Mater.* 37, 706 (2014).
- [13] F. Tang, Y. Cao, W. Guo, Y. Chen, J. Huang, Z. Deng, Z. Liu, and Z. Huang, *Opt. Mater.* 33, 1278 (2011).
- [14] C. Sallé, A. Maître, J.-F. Baumard, and Y. Rabinovitch, *Optical Review* 14, 169 (2007).
- [15] R. Boulesteix, A. Maître, J.-F. Baumard, Y. Rabinovitch, C. Sallé, S. Weber, and M. Kilo, *J. Eur. Ceram. Soc.* 29, 2517 (2009).
- [16] R. Boulesteix, A. Maître, J.-F. Baumard, C. Sallé, and Y. Rabinovitch, *Opt. Mater.* 31, 711 (2009).
- [17] H. Van Dijk, *Mater. Res. Bull.* 19, 1669 (1984).
- [18] A. Ikesue, K. Yoshida, T. Yamamoto, and I. Yamaga, *J. Am. Ceram. Soc.* 80, 1517 (1997).
- [19] S. Kochawattana, A. Stevenson, S.-H. Lee, M. Ramirez, V. Gopalan, J. Dumm, V. K. Castillo, G. J. Quarles, and G. L. Messing, *J. Eur. Ceram. Soc.* 28, 1527 (2008).
- [20] G. Phillipps and J. Vater, *Appl. Opt.* 32, 3210 (1993).
- [21] S. H. Lee et al., *J. Am. Ceram. Soc.* 92, 1456 (2009).
- [22] K. Fujioka, A. Sugiyama, Y. Fujimoto, K. Kawanaka, and N. Miyana, in *9th Laser Ceramics Symposium*, Daejeon, Korea (2013).
- [23] M. Suárez, A. Fernández, J. Menéndez, M. Nygren, R. Torrecillas, and Z. Zhao, *J. Eur. Ceram. Soc.* 30, 1489 (2010).
- [24] A. J. Stevenson, E. R. Kupp, and G. L. Messing, *J. Mater. Res.* 26 (2011).
- [25] R. R. Tummala, *J. Am. Ceram. Soc.* 74, 895 (1991).
- [26] H. S. Jadhav, M.-S. Cho, R. S. Kalubarme, J.-S. Lee, K.-N. Jung, K.-H. Shin, and C.-J. Park, *J. Power Sources* 241, 502 (2013).
- [27] P. James and W. Shi, *J. Mater. Sci.* 28, 2260 (1993).
- [28] K. Tsukuma, *J. Ceram. Soc. Jpn.* 114, 802 (2006).
- [29] L. Moreira, L. Ponce, E. de Posada, T. Flores, Y. Peñaloza, O. Vázquez, and Y. Pérez, *Ceram. Int.* 41, 11786 (2015).
- [30] A. Ikesue and K. Kamata, *J. Am. Ceram. Soc.* 79, 1927 (1996).
- [31] M. I. Mendelson, *J. Am. Ceram. Soc.* 52, 443 (1969).
- [32] A. Ikesue, T. Kinoshita, K. Kamata, and K. Yoshida, *J. Am. Ceram. Soc.* 78, 1033 (1995).
- [33] O. Fabrichnaya, H. Jürgen Seifert, R. Weiland, T. Ludwig, F. Aldinger, and A. Navrotsky, *Z. Metallkd* 92, 1083 (2001).
- [34] A. Maître, C. Sallé, R. Boulesteix, J. F. Baumard, and Y. Rabinovitch, *J. Am. Ceram. Soc.* 91, 406 (2008).
- [35] M. Liu, S. Wang, D. Tang, L. Chen, and J. Ma, *Sci Sinter* 40, 311 (2008).
- [36] J. Zhou et al., *Ceram. Int.* 37, 119 (2011).
- [37] Y. Shan, J. Xu, G. Wang, X. Sun, G. Liu, J. Xu, and J. Li, *Ceram. Int.* 41, 3992 (2015).
- [38] A. Belyakov and A. Sukhozhak, *Glass Ceram.* 52, 14 (1995).
- [39] G. Wildlic, *Chinese Light Industry Publisher*, 20 (1980).
- [40] D. Taylor, D. Dent, D. Braski, and B. Fabes, *J. Mater. Res.* 11, 1870 (1996).
- [41] O. H. Kwon and G. L. Messing, *Acta Metall. Mater.* 39, 2059 (1991).